Comprehensive multifractal analysis of turbulent velocity using wavelet leaders

Bruno Lashermes, Stéphane Roux, Patrice Abry, Stéphane Jaffard

HAL Id: hal-00798403
https://hal.science/hal-00798403

Submitted on 8 Mar 2013

Comprehensive Multifractal Analysis of Turbulent Velocity Using the Wavelet Leaders

Bruno Lashermes[1], Stéphane Roux[2], Patrice Abry[2], and Stéphane Jaffard[3]

[1] St Anthony Falls Laboratory and National Center for Earth-surface Dynamics, Dept. of Civil Engineering, University of Minnesota
2 3rd Ave S - Minneapolis, MN, 55414 - USA
[2] Laboratoire de Physique, École Normale Supérieure de Lyon and CNRS
46, allée d'Italie - 69007 Lyon - France
[3] Laboratoire d'Analyse et de Mathématiques Appliquées, Université Paris XII and Institut Universitaire de France
61, avenue du Général de Gaulle - 94010 Créteil - France

the date of receipt and acceptance should be inserted later

Abstract. The multifractal (MF) framework relates the scaling properties of turbulence to its local regularity properties through a statistical description as a collection of local singularities. The MF properties are moreover linked to the multiplicative cascade process that creates the peculiar properties of turbulence such as intermittency. A comprehensive estimation of the MF properties of turbulence from data analysis, using a tool valid for all kind of singularities (including oscillating singularities) and mathematically well-founded, is thus of first importance in order to extract a reliable information on the underlying physical processes. The MF formalism based on the wavelet leaders (WL) is a new MF formalism which is the first to meet all these requests. This paper aims at its description and at its application to experimental turbulent velocity data. After a detailed discussion of the practical use of the MF formalism based on the WL the following questions are carefully investigated: (1) What is the dependence of MF properties on the Reynolds number? (2) Are oscillating singularities present in turbulent velocity data? (3) Which MF model does correctly account for the observed MF properties? Results from several data set analyses are used to discuss the dependence of the computed MF properties on the Reynolds number but also to assess their common or universal component. An exact though partial answer (no oscillating singularities are detected) to the issue of the presence of oscillating singularities is provided for the first time. Eventually an accurate parameterization with cumulants exponents up to order 4 confirms that the log-normal model (with $c_2 = -0.025 \pm 0.002$) correctly accounts for the universal MF properties of turbulent velocity.

PACS. XX.XX.XX No PACS code given

1 Introduction

Turbulent velocity and multifractal description.
The streamwise component of turbulent flow velocity spatial field is known to exhibit a main feature: very irregular fluctuations over a large range of scales, which statistical moments furthermore behave within the so-called inertial scale range like power laws with respect to the scale a:

$$< |v(x_0 + a) - v(x_0)|^q > \quad \sim \quad a^{\zeta(q)} \qquad (1)$$

where $< . >$ denotes the spatial averaging over the locations x_0. The $\zeta(q)$ are called the scaling exponents. Characterization and understanding of the observed scaling properties play a central role in the theoretical description of turbulence, following the seminal work by Kolmogorov in 1941 [1] in which were predicted linear scaling exponents: $\zeta(q) = q/3$. This prediction was actually lacking of consistency and have been refined by Obukhov and Kol-

mogorov in 1962 [2,3] who predicted a (quadratic) non-linear behavior of the scaling exponents. The non-linear behavior of the $\zeta(q)$ was confirmed by various experimental results and other $\zeta(q)$ models have been also proposed (see [4] for an overview). The non-linear behavior of the $\zeta(q)$ mainly received interpretation through the existence of an underlying multiplicative cascade structure of the energy dissipation field [5,6] (according to the early heuristics from Richardson [7]) which results in a multiplicative cascade structure of the velocity fluctuations [8].

The MF framework relates the scaling properties to the local regularity properties by describing the turbulent velocity field as a collection of local singularities (roughly speaking simple singularities: $|x - x_0|^h$ or oscillating singularities: $|x - x_0|^h \sin\left(1/|x - x_0|^\beta\right)$ which local regularity is characterized by the exponent h) which are distributed on interwoven fractal sets. The local regularity receives a proper definition with the Hölder exponent and the MF

analysis aims at characterizing the spatial distribution of the Hölder exponents with the so-called singularity spectrum $D(h)$. Though many MF models of turbulence implicitly involve only simple singularities and in spite of several works [9–12], the existence of oscillating singularities in turbulent velocity data remains an open issue.

Practical multifractal analysis.   One of the main goals of numerical analysis of experimental turbulent velocity data is the measurement of the MF properties, i.e., the singularity spectrum $D(h)$, for instance to discriminate between the various proposed MF models. The singularity spectrum can be (at least partially) computed from real data using a MF formalism (firstly introduced in the mid 80's [13]) which relates the $\zeta(q)$ to $D(h)$ through the Legendre transform.

Development of the wavelet transforms allowed real enhancements in various fields of signal processing [14], for instance the improvement of the MF formalisms [15–17]. The MF formalisms based on either the increment or the wavelet coefficients suffer anyway from a common drawback: the $\zeta(q)$ with negative orders q and hence the right part of $D(h)$ can not be computed. The WTMM (Wavelet Transform Modulus Maxima) MF formalism has been heuristically introduced in order to overcome this failure [15,18,19]. This formalism has been checked to compute the whole singularity spectrum on a selection of synthetic MF processes with simple singularities but still doesn't receive a theoretical proof.

Moreover, in spite of several works [11,12] the effect of oscillating singularities on the use of MF formalisms is badly understood but is known to possibly result in the failure of the MF formalisms based on the wavelet coefficients [17].

Wavelet leaders.   The WL are multi-resolution coefficients defined from a specific wavelet transform (the discrete wavelet transform) which have recently been introduced in order to define a MF formalism allowing a comprehensive MF analysis (measurement of the whole singularity spectrum) relying on a mathematically well-founded basis [20]. The WL provide a characterization more appropriated to the derivation of a MF formalism than the wavelet coefficients. As a consequence the MF formalism based on the WL is proven to be valid for functions with all kinds of singularities (including oscillating singularities) whereas the one based on the wavelet coefficients is known to fail.

This new MF formalism has been implemented and numerically characterized on synthetic MF data in [21–23]. Its application to experimental turbulent velocity data is the aim of this paper and we think that the unique properties of the MF formalism based on the WL (complete MF analysis relying on theoretical basis and validity for all kind of singularities) indeed bring interesting and new results on the MF description of turbulent velocity.

Outline.   This paper is organized as follows. Section 2 provides a presentation of the MF framework for func-

tions. Precise definitions of pointwise regularity, Hölder exponent and singularity spectrum are displayed before an overview of the classical ways to perform a practical MF analysis: the MF formalism and the cumulant analysis. Section 3 discusses the important choice of multiresolution coefficients, introduces the WL and the derived MF formalism. The validity of this last is stated and compared to former MF formalisms one and illustrated using toy-examples. Section 4 discusses the use of MF description in the turbulence field as well as the underlying assumptions. Practical MF analysis of several experimental turbulent velocity data sets using the WL is then performed in Section 5 and all different steps are carefully discussed. Results from experimental data analysis are compared to previous results and conclusions about the MF properties of turbulent velocity are eventually drawn and discussed. Final conclusions are given in Section 6.

2 Multifractal framework

The MF framework is a statistical description of a function f through its pointwise (or local) regularity properties (see [17,23] for a thorough introduction).

2.1 Multifractal analysis

2.1.1 Hölder exponent

The pointwise regularity of a function f at point x_0 is properly defined by the *Hölder exponent* $h(x_0)$ (the following definition actually holds for $h < 1$ only but easily extends to $h \geq 1$):

$$h(x_0) = \mathrm{Sup}\left\{\alpha : \ f \in C^\alpha(x_0)\right\}, \tag{2}$$

where

$$f \in C^\alpha(x_0) \text{ if } |x - x_0| \leq \epsilon, \ |f(x) - f(x_0)| \leq C|x - x_0|^\alpha. \tag{3}$$

The value of the Hölder exponent is interpreted as follows: the closer to 0 $h(x_0)$ is, the more irregular (or singular) at point x_0 the function is. In contrast, a larger value of $h(x_0)$ is related to a smoother (more regular) behavior at x_0.

2.1.2 Simple and oscillating singularities

A specific value $h(x_0)$ for the Hölder exponent at point x_0 does not imply a local power law behavior (*simple singularity* or *cusp*):

$$|f(x) - f(x_0)| \simeq b|x - x_0|^{h(x_0)} \tag{4}$$

when $x \to x_0$. Other local singular behaviors indeed result in the same value for the Hölder exponent, for instance an *oscillating singularity* (or *chirp*):

$$|f(x) - f(x_0)| \simeq b|x - x_0|^{h(x_0)} \sin\left(\frac{1}{|x - x_0|^{\beta(x_0)}}\right) \tag{5}$$

when $x \to x_0$. $\beta(x_0)$ is called the *oscillating exponent.*

The local regularity properties cannot thus be extensively characterized with simple singularities only and a comprehensive MF analysis has to take into account all possible local behaviors such as oscillating singularities.

2.1.3 Singularity spectrum

The points x_0 associated to a specific Hölder exponent value h are distributed on interwoven fractal subsets $E(h)$:

$$E(h) = \{x_0 : h(x_0) = h\}. \tag{6}$$

The MF description provides an efficient characterization of MF functions through a hierarchical classification of the subsets $E(h)$ using their Hausdorff dimension (see for instance [24]):

$$D(h) = \text{Dim}_H E(h). \tag{7}$$

(By convention $\text{Dim}_H E = -\infty$ if E is the empty set.)

The function $D(h)$ is called the *singularity spectrum* and its estimation is the goal of MF analysis. The singularity spectrum has been shown to be a relevant quantity to characterize stochastic processes in nature (for instance in turbulence, see [4]) since it is related to the underlying statistical structure of data fluctuations.

Monofractal functions are a specific subclass of MF functions for which the Hölder exponent takes an unique value H at every point x_0. The singularity spectrum then reduces to a single point: $D(h) = 1$ if $h = H$ and $D(h) = -\infty$ if $h \neq H$. A well known example of monofractal processes is the fractional Brownian motion which has been proposed by Kolmogorov in 1941 [25] to model turbulent velocity, with $H = 1/3$. In contrast a function is multifractal if the Hölder exponent can take different values: its singularity spectrum thus takes finite values on an interval $[h_{min}, h_{max}]$ with $h_{max} > h_{min}$. For most multifractal functions the singularity spectrum $D(h)$ is a concave function which is bell-shaped (see Fig. 7 for instance). $D(h)$ then reaches its maximum at an abscissa h_0 and the *left* (*right*) part of the singularity spectrum is defined in this paper as the part of $D(h)$ for which $h \leq h_0$ ($h \geq h_0$).

2.2 Multifractal formalisms

2.2.1 Structure functions and scaling exponents

MF analysis is performed on data with specific tools, the MF formalisms. The singularity spectrum $D(h)$ is estimated from the statistics of the local fluctuations $c(x_0, a)$ of the function at different scales a and at different locations x_0. The archetypal choice [13] for the local fluctuations (or multi-resolution coefficients) $c(x_0, a)$ is the increment coefficients:

$$c(x_0, a) = \delta(x_0, a) = f(x_0 + a) - f(x_0). \tag{8}$$

The issue of the choice of multi-resolution coefficients will be addressed in Section 3.1.

The *structure functions* $S(q, a)$ are defined as estimates (by space-averaging) of the q-th statistical moments of the absolute value of the $c(x_0, a)$ at scale a:

$$S(q, a) = \frac{1}{n(a)} \sum_{x_0} |c(x_0, a)|^q \tag{9}$$

where $n(a)$ is the number of coefficients $c(x_0, a)$ available at scale a.

The structure functions behave like power laws for MF functions when $a \to 0$:

$$S(q, a) \sim a^{\zeta(q)}, \tag{10}$$

defining the usual *scaling exponents* $\zeta(q)$, indexed by order q.

2.2.2 Multifractal formalisms

The MF formalisms state that the scaling exponents $\zeta(q)$ relate to the singularity spectrum $D(h)$ through a *Legendre transform*:

$$D(h) = 1 + \min_q [qh - \zeta(q)]. \tag{11}$$

The Legendre transform link between the scaling exponents and the singularity spectrum can be heuristically understood as follows (this is not a formal proof). Since the Hausdorff dimension of the subset $E(h)$ is $D(h)$, the number of multi-resolution coefficients, which typical size is the scale a, needed to cover $E(h)$ is proportional to $a^{1-D(h)}$ when $a \to 0$. If $c(x_0, a) \sim a^h$ when $a \to 0$, the contribution of a specific Hölder exponent h to $S(q, a)$ is thus:

$$\sim a^{1-D(h)} a^{qh} = a^{1+qh-D(h)}. \tag{12}$$

For a given order q the contribution of the Hölder exponent value h such that $1 + qh - D(h)$ is minimal becomes predominant when $a \to 0$:

$$S(q, a) \sim a^{1+\min_h(qh-D(h))}, \tag{13}$$

leading to the identification:

$$\zeta(q) = 1 + \min_h [qh - D(h)]. \tag{14}$$

In turns, since the inverse of the Legendre transform of a concave function is the Legendre transform, one may expect (11).

Note that Eq. (14) implies a linear behavior of the scaling exponents for monofractal functions (cf., Section 2.1.3): $\zeta(q) = qH$ and a non-linear behavior for multifractal functions.

The MF formalism is valid if the Legendre transform of the scaling exponents is equal to the singularity spectrum. Eq. (11) is indeed not a theoretical result and the Legendre transform of the scaling exponents may depart from the singularity spectrum. The validity of a MF formalism actually depends on the specific choice of the multi-resolution coefficients $c(x_0, a)$. This is one of the key-point discussed all along this paper.

2.2.3 Cumulant analysis

A parametrical characterization of the singularity spectrum $D(h)$ can be performed using the so-called cumulant analysis method, which is a tool used in turbulence [26, 27] and in other fields [28,29]. This method provides estimates of the parameters c_p of the Taylor series expansion of $\zeta(q)$ for $q \to 0$ [1]:

$$\zeta(q) = \sum_{p \geq 1} \frac{c_p}{p!} q^p. \qquad (15)$$

The estimation of the c_p is performed by computing (with spatial averaging) the cumulants $C(p,a)$ of order p of the logarithm of the absolute value of the multi-resolution coefficients $c(x_0, a)$ at a given scale a. The cumulants $C(p,a)$ are linear functions of $\ln a$ for MF functions when $a \to 0$. For instance for $p = 1$ and 2:

$$C(1,a) = \frac{1}{n(a)} \sum_{x_0} \ln |c(x_0,a)| \simeq b_1 + c_1 \ln a \qquad (16)$$

$$C(2,a) = \frac{1}{n(a)} \sum_{x_0} [\ln |c(x_0,a)| - C(1,a)]^2 \simeq b_2 + c_2 \ln a. \qquad (17)$$

Linear regressions of $C(p,l)$ versus $\ln a$ thus allow estimation of the c_p, called the *cumulant exponents*.

The cumulant analysis is an alternative way of performing MF analysis, which main interest is to provide a concise parameterization of the singularity spectrum $D(h)$. If the process under analysis is monofractal then $c_1 = H \neq 0$ and $c_p = 0$ for $p > 1$. A non-zero value for c_2 explicitly establishes the multifractal (vs. monofractal) nature of the data and the parameter c_2 (also called the intermittency coefficient) is used to characterize the degree of multifractality. Indeed, a quadratic approximation of the scaling exponents: $\zeta(q) \simeq c_1 q + c_2 q^2/2$ (when $q \to 0$) which corresponds to a quadratic approximation of the singularity spectrum: $D(h) \simeq 1 + \frac{(h-c_1)^2}{2c_2}$ (when $h \to c_1$) is a commonly used MF model (see Section 4.1).

3 Multifractal formalism based on the wavelet leaders

3.1 Choice of multi-resolution coefficients

The specific choice of the multi-resolution coefficients $c(x_0, a)$ plays a central role for the validity of MF formalisms. The wavelet transforms (see [14] for an overview) provide a more versatile and efficient choice for multi-resolution coefficients (see for instance [19,17]) than the original increments coefficients [13]. The MF formalisms based on the increment or wavelet coefficients anyway share a common and major drawback: they fail to compute the right part of the singularity spectrum, which is

associated to the scaling exponents with negative order value. Since the cumulant exponents c_p are defined as the Taylor expansion of $\zeta(q)$ for $q \to 0$ (cf., Section 2.2.3), they are sensitive to the $\zeta(q)$ with $q > 0$ and $q < 0$ and thus are poorly estimated. Moreover the increment or wavelet coefficients do not provide a correct characterization of the pointwise regularity properties of data with oscillating singularities and may thus yield erroneous results even for the left part of the singularity spectrum. These drawbacks are thoroughly illustrated in Section 3.3 using the discrete wavelet coefficients[2].

The WTMM methodology[3] is a MF formalism, based on multi-resolution coefficients defined from the continuous wavelet transform, which has been heuristically introduced in order to compute the right part of the singularity spectrum. It has been numerically shown to indeed compute the whole singularity spectrum of a selection of synthetic MF processes with simple singularities only. But it does not address the issue of oscillating singularities and furthermore does not receive any mathematical basis.

The wavelet leaders (WL) are multi-resolution coefficients recently introduced [20] and numerically characterized [21–23] in order to build a MF formalism which relies on exact theoretical results and is able to compute the whole singularity spectrum of functions with all kind of singularities. The presentation and the characterization of the WL and the related MF formalism, and its application to experimental turbulent velocity data are the goals of this paper.

3.2 The wavelet leaders

3.2.1 Discrete wavelet coefficients

The WL are defined from the discrete wavelet coefficients (hereafter DWC). The discrete wavelet transforms (see [14] for an overview) is a decomposition (also called multi-resolution analysis) of the function f on the orthogonal basis $\{\psi_{j,k}\}_{j \in \mathbb{Z}, k \in \mathbb{Z}}$ composed of the discrete wavelets $\psi_{j,k}$:

$$d(j,k) = \int_{\mathbb{R}} dx \, \psi_{j,k}(x) f(x) \qquad (18)$$

with:

$$\int_{\mathbb{R}} dx \, \psi_{j,k}(x) \psi_{j',k'}(x) = 0 \quad \text{if } (j,k) \neq (j',k') \qquad (19)$$

The integers $j \in \mathbb{Z}$ and $k \in \mathbb{Z}$ index the scale $a = 2^j$ and the location $x_0 = k2^j$. The wavelets $\{\psi_{j,k}\}_{j \in \mathbb{Z}, k \in \mathbb{Z}}$

---

[1] Note the coefficient corresponding to $p = 0$ is necessarily zero since $\zeta(0) = 0$ (see Eq. (9)).

[2] The wavelet transforms divide between the discrete and the continuous wavelet transforms and both of them provide the same characterization of pointwise regularity properties: the related MF formalisms have thus equivalent validity properties [17].

[3] The reader is referred to [15,18,19,28] for detailed presentation and illustration of this MF formalism.

are space-shifted and scale-dilated templates of a mother-wavelet ψ_0:

$$\psi_{j,k}(x) = \frac{1}{2^j}\psi_0\left(\frac{x - k2^j}{2^j}\right) \qquad (20)$$

and define a basis distributed according to a dyadic basis in the space-scale plane (cf., Fig. 1). Every wavelet $\psi_{j,k}$ and then every DWC $d(j,k)$ can be associated to the dyadic interval $\lambda(j,k)$:

$$\lambda(j,k) = [2^j k, 2^j(k+1)[\qquad (21)$$

which will be usefully used for indexing the DWC: $d(j,k) = d(\lambda)$.

3.2.2 Definition of the wavelet leaders

The wavelet leaders are defined from the DWC as follows:

$$l(j,k) = \sup_{\lambda' \subset 3\lambda(j,k), \ j' \leq j} |d(\lambda')| \qquad (22)$$

with $3\lambda(j,k) = \lambda(j, k-1) \cup \lambda(j,k) \cup \lambda(j, k+1)$. The WL $l(j,k)$ associated to the scale 2^j and to the location $k2^j$ is then the supremum of the absolute value of the DWC $d(j,k)$ corresponding to the same and adjacent locations $(k2^j, (k-1)2^j$ and $(k+1)2^j)$ and to the same and smaller scales ($j' \leq j$) as sketched in Fig. 1.

3.2.3 Characterization of pointwise regularity

If $h(x_0)$ is the Hölder exponent of f at x_0 then one has[4]:

$$\forall j, \ l(k,j) \sim C2^{jh(x_0)}, \qquad (23)$$

with the WL (where k is chosen such that $x_0 \in \lambda(j,k)$ and C is a positive constant) whereas one only has:

$$\forall j, \ |d_f(k,j)| \sim C2^{jh(x_0)}\left(1 + \left|2^{-j}x_0 - k\right|^{h(x_0)}\right), \quad (24)$$

with the DWC (note that the last characterization is a general feature of wavelet coefficients and is not specific to the DWC).

The WL characterize the local regularity with a local power law behavior (with exponent $h(x_0)$) whereas the DWC offer a power law characterization which can be perturbed by a multiplicative term. The WL thus provide a characterization of the pointwise regularity which is better suited to the derivation of a MF formalism than the one based on the DWC since the derivation mainly relies on the assumption that the chosen multi-resolution coefficients do locally behave as power laws with exponent $h(x_0)$ (see the heuristic argument in 2.2.2).

---

[4] The notation $a \sim b$ means that the lower limit of $\log(a)/\log(b)$ is 1.

3.3 Validity of multifractal formalisms based on the DWC and the WL

3.3.1 Theoretical results

Exact results proved in [20,23] are stated in this section. Quantities X will be denoted X^d when computed with the DWC and X^l when computed with the WL. $LT[X](h)$ denotes the Legendre transform of $X(q)$.

If f is an uniform Hölder function[5] with a concave[6] singularity spectrum, then the MF formalism based on the WL is *exact*:

$$\forall h, \quad LT[\zeta^l](h) = D(h) \qquad (25)$$

and thus achieves the goal of the MF analysis, i.e., the exact computation of the whole singularity spectrum.

The MF formalism based on the DWC also receives exact results [17,20]. Let us recall that h_0 is defined as the abscissa of the maximum of the singularity spectrum $D(h)$ (cf., Section 2.1.3) and define h_c such that $q_c h_c = D(h_c)$ and $q_c = \frac{dD}{dh}(h_c)$, i.e., h_c is the abscissa at which the tangent of $D(h)$ is drawn from the origin $(h, D) = (0, 0)$ (cf., Fig. 2. If f is an uniform Hölder function with a concave singularity spectrum, then:

$$\text{if } h \leq h_c, \quad LT[\zeta^d](h) = D(h), \qquad (26)$$

and if f has furthermore only simple singularities:

$$\text{if } h \leq h_0, \quad LT[\zeta^d](h) = D(h). \qquad (27)$$

Use of this formalism can hence only provide measurement of the left part of $D(h)$ if simple singularities only are present, and even of a smaller part of it if oscillating singularities are present. In other words the right part of $D(h)$ can not be estimated with the DWC and the computation of the left part itself can even fail as a result of the presence of oscillating singularities.

The formalism based on the WL then brings a real quantitative enhancement: it yields a comprehensive MF analysis, i.e., the computation of the whole singularity spectrum $D(h)$ ($\forall h$) regardless of whether simple singularities are the only ones present or not. These results are sketched in Fig. 2. In addition to that, we point out that it relies on mathematically well-fonded basis, in contrast to the WTMM methodology for which no exact result exists (though its validity has been numerically checked with synthetic MF processes with simple singularities).

Eventually note that if f is only uniform Hölder (i.e., with a non-concave singularity spectrum), all the results shown above weakens into an upper bound. For instance (25) is turned to:

$$\forall h, \quad LT[\zeta^l](h) \leq D(h). \qquad (28)$$

---

[5] A function f is uniform Hölder of order $\alpha < 1$ ($f \in C^\alpha(\mathbb{R})$) if $\exists C > 0: \quad \forall x_0, \quad |f(x) - f(x_0)| \leq C|x - x_0|^\alpha$. This definition easily extends to $\alpha \geq 1$.

[6] A function is concave if $\forall \ x, y$ with $t \in [0,1]$, then $f(tx + (1-t)y) \geq tf(x) + (1-t)f(y)$.

Even though there exists some counter-examples, the main majority of singularity spectra used to model physical processes (for instance all models used in turbulence [4]) or to define synthetic data corresponds to concave functions. This last case will not be further discussed and all singularity spectra considered in the sequel will be assumed to be concave.

3.3.2 Illustration #1: oscillating singularities

The WL always characterize the local regularity with a local power law behavior (with exponent $h(x_0)$) whereas the DWC offer a power law characterization which can be perturbed by a multiplicative term (cf., Eqs. (23) and (24)). This difference is illustrated in Fig. 3 where the $d(j, k)$ and $l(j, k)$ are computed for an isolated simple singularity (with $h = 0.6$) and an isolated oscillating singularity (with $(h, \beta) = (0.6, 1)$). The WL exhibit a power law behavior with the correct exponent both for the cusp and the chirp whereas the DWC behave like a power law (with the correct exponent) only for the cusp. Since the validity of a MF formalisms mainly relies on the assumption that the associated multi-resolution coefficients do locally behave as power laws with exponent $h(x_0)$ (cf., Section 3.2.3), this simple example clearly points out at the failure of the MF formalism based on the DWC[7] to correctly compute the singularity spectrum of functions with oscillating singularities when $h_c \leq h \leq h_0$.

3.3.3 Illustration #2: scaling exponents with negative orders and the right part of the singularity spectrum

The right part of $D(h)$ (cf., Section 2.1.3) is related to the scaling exponents $\zeta(q)$ with negative order ($q < 0$). The $\zeta(q)$ are defined from the structure functions $S(q, a)$ which are the estimates (by space-averaging) of the q-th order statistical moments of the $c(x_0, a)$ (cf., Eq. (9)). A meaningful estimation of the statistical moments of the $c(x_0, a)$ with a negative order implies that at least the chosen $c(x_0, a)$ have a probability distribution function which is zero-valued for $c(x_0, a) = 0$.

The random wavelet cascade process is a synthetic MF process commonly used to benchmark MF formalisms (see for instance [21–23]) and model turbulent velocity (see [30] for a thorough definition) and which MF properties can be easily prescribed. The histograms of the absolute value of the DWC and the WL computed on a realization of thi process are plotted in Fig. 4 and show that the computation of statistical moments of the $d(j, k)$ with negative order is meaningless in contrast of those of the $l(j, k)$. This clearly illustrates that the MF formalism based on the DWC fails to provide the right part of the singularity spectrum since not being able to compute the scaling exponents with negative order.

3.4 Detection of oscillating singularities

In spite of various attempts [9–12] the detection of oscillating singularities remains an important issue in signal processing. This section points out that the failure of the MF formalism based on the DWC when performing a MF analysis of data with oscillating singularities can be actually useful. Indeed, since the MF formalism based on the WL is expected to be valid in the same situation, a discrepancy between the results given by these two formalisms in the range $[h_c, h_0]$ is a signature of the presence of oscillating singularities.

In turn it is worth noting that an agreement of the results between the two MF formalisms should not be taken as a proof of the absence of oscillating singularities. The two formalisms might indeed give coinciding results if oscillating singularities exist but bring a *minor* contribution to the singularity spectrum. Let us first define $D(h, \beta)$ (called the grand-canonical spectrum [11,12]) as the Hausdorff dimension of the subset of points x_0 at which the Hölder and oscillating exponents takes the specific values h and β (see Eq. (5))[8]. The singularity spectrum $D(h)$ then straightforwardly relates to $D(h, \beta)$:

$$D(h) = \sup_\beta D(h, \beta).$$

If $D(h) = D(h, \beta)$ with $\beta = 0$ the oscillating singularities bring a *minor* contribution to $D(h)$ since the simple singularities ($\beta = 0$) with Hölder exponent value h are spatially distributed on a subset with a larger Hausdorff dimension than the ones characterizing the oscillating singularities ($\beta \neq 0$) with the same Hölder exponent value.

The exact behavior of the MF formalism based on the DWC for data with oscillating singularities that bring a minor contribution to $D(h)$ is still not fully understood [32] and is under current investigation. This topic is then not further discussed in this paper and the following partial but cautious conclusion is drawn: if an agreement between the Legendre transforms of the $\zeta^d(q)$ of the $\zeta^l(q)$ is observed for $h_c \leq h \leq h_0$, there is either no oscillating singularities or oscillating singularities that bring a minor contribution to the singularity spectrum $D(h)$. In turns a discrepancy between the results of the two MF formalisms in that range proves the presence of oscillating singularities.

4 Multifractality and turbulence

4.1 Multifractal models

Several MF models have been proposed for the Eulerian turbulent velocity (see [4] for an overview). The two most commonly used are the log-normal model (after the work by Obukhov and Kolmogorov [2,3]) and the She-Lévêque model [33] which both relate to a multiplicative cascade process down the scales (both models can be seen as two

---

[7] This is actually a general result valid for all wavelet coefficients, either discrete or continuous, and also for increments coefficients.

[8] Proper definition of the oscillating exponent β exists [31] but is not discussed here.

specific cases of the more general framework of the infinitely divisible cascades [8,34,35]). The MF properties of these processes are controlled by the statistics of the multipliers: the log-normal model corresponds to log-normal statistics whereas the She-Lévêque model corresponds to log-Poisson statistics [36]. It is noted that both models predict MF functions with simple singularities only.

The log-normal model predicts quadratic expressions for both the scaling exponents and the singularity spectrum:

$$D_{ln}(h) = \begin{cases} 1 + \frac{(h-c_1)^2}{c_2} & \text{if } h_*^+ \leq h \leq h_*^- \\ -\infty & \text{else} \end{cases}, \quad (29)$$

$$\zeta_{ln}(q) = \begin{cases} c_1 q + \frac{c_2}{2} q^2, & q_*^- \leq q \leq q_*^+ \\ 1 + q h_*^-, & q \geq q_*^+ \\ 1 + q h_*^+, & q \leq q_*^- \end{cases} \quad (30)$$

with $c_1 = 1/3 - 3c_2/2$ (so that $\zeta_{ln}(3) = 1$) while the She-Lévêque model predicts:

$$D_{SL}(h) = \begin{cases} \left(h - \frac{1}{9}\right)\left[A_1 - A_2 \ln\left(h - \frac{1}{9}\right)\right] - 2 \\ \qquad\qquad\qquad \text{if } h_*^+ \leq h \leq h_*^- \\ -\infty \qquad\qquad\qquad\qquad\quad \text{else} \end{cases} \quad (31)$$

$$\zeta_{SL}(q) = \begin{cases} \frac{q}{9} + 2\left[1 - \left(\frac{2}{3}\right)^{q/3}\right], & q_*^- \leq q \leq q_*^+ \\ 1 + q h_*^-, & q \geq q_*^+ \\ 1 + q h_*^+, & q \leq q_*^- \end{cases} \quad (32)$$

with $A_1 = 3\left(\frac{1+ln(ln(\frac{3}{2}))}{ln(\frac{3}{2})} - 1\right)$, $A_2 = \frac{3}{ln(\frac{3}{2})}$. (The reader can refer to [37,21,38] for a thorough discussion of the linear behavior of the scaling exponents beyond the critical orders q_*^+ and q_*^-.) The critical parameters h_*^+, h_*^-, q_*^+ and q_*^- are for the log-normal model:

$$h_*^+ = c_1 - \sqrt{-2c_2}, \quad h_*^- = c_1 + \sqrt{-2c_2},$$

$$q_*^+ = -q_*^- = \sqrt{-2/c_2}$$

and for the She-Lévêque model:

$$h_*^+ \simeq 0.162, \quad h_*^- \simeq 0.694,$$

$$q_*^- \simeq -5.69, \quad q_*^+ \simeq 12.36.$$

The log-normal model has one free parameter, the intermittency coefficient c_2 (which coincides with the second order cumulant exponent), which commonly accepted value is $c_2 = -0.025$ [39–41,27] (the She-Lévêque model has no free parameter). Both models are multifractal models (as opposed to monofractal ones) and the corresponding cumulants exponents are listed in Table 2. The scaling exponents and the singularity spectra predicted by these models are plotted in Fig. 6 and Fig. 7. It is noted that the predictions for the left part of the singularity spectrum (or the scaling exponents with positive order) are numerically very close whereas they clearly differ for the right part of $D(h)$ (or $\zeta(q)$ with $q > 0$). This remark illustrates the importance of designing tools allowing a complete MF analysis, i.e., the computation of both the left and the right part of the singularity spectrum.

4.2 Multifractality and universality

Let us discuss an important assumption of the MF description of turbulence. A turbulence experiment is necessarily characterized by a finite Reynolds number R_λ [9] and the large fluctuations observed at the inertial scales are smoothed out at smallest scales by the viscous forces (which become predominant at the Kolmogorov scale): the velocity spatial profiles are not locally singular (they possess at least a first order derivative at every point). The MF description (and thus the associated singularity spectrum models) actually relates to the pointwise regularity properties of the turbulent velocity in the limit of infinite Reynolds numbers: $R_\lambda \to +\infty$. In other words it is assumed that the scaling properties observed at the inertial scales extend down to all smallest scales, i.e., $a \to 0$, and thus that velocity has the pointwise regularity properties characterized by the singularity spectrum $D(h)$ associated to these scaling properties. This assumption is entirely consistent since the same mechanism (a multiplicative cascade through the scales) is used to model both the scaling properties of the structure functions and the (asymptotic) pointwise regularity properties.

All theoretical predictions about the singularity spectrum of turbulent velocity thus implicitly concern the limit $R_\lambda \to +\infty$. This is a universal description of turbulence since the statistical properties of any turbulent flow (turbulent jet, grid turbulence, ...) are expected to coincide in that limit: all turbulent flows are hence characterized by common scaling exponents $\zeta(q)$ and singularity spectrum $D(h)$. The value of $\zeta(3)$ is for instance predicted by the Kolmogorov's four fifths law [25] (derived from the Kármán-Howarth equation [42]) which is an exact result for any turbulent flow in the limit of $R_\lambda \to +\infty$: the third order structure function is an exact power law with scaling exponent $\zeta(3) = 1$.

It is known that the scaling exponent $\zeta(3)$ computed from experimental data departs from 1 and does not take the same value for all experiments, which is also true for any other value of the order q. It is known as well (see for instance [43]) that the *normalized scaling exponents*:

$$\tilde{\zeta}(q) = \frac{\zeta(q)}{\zeta(3)} \quad (33)$$

(which necessarily take the specific value: $\tilde{\zeta}(3) = 1$) do collapse on a common curve for different experiments, supporting the fact that the *normalized* scaling exponents $\tilde{\zeta}(q)$ (and thus their Legendre transform $\tilde{D}(h)$) are universal in contrast to the *raw* scaling exponents $\zeta(q)$ (this will be illustrated in Section 5.4.1). Results about universal scaling and/or MF properties of turbulence are hence usually discussed using the $\tilde{\zeta}(q)$ and not the $\zeta(q)$. Note that the coefficients of the Taylor series expansion of $\tilde{\zeta}(q)$ around

---

[9]   The Taylor scale based Reynolds number, called Reynolds number in the sequel, is defined as: $R_\lambda = \frac{\sigma\lambda}{\nu}$ where σ is the standard deviation of the velocity $v(x)$, $\lambda = \sqrt{\frac{\sigma^2}{\mathbb{E}(\frac{\partial v}{\partial x})^2}}$ is the so-called Taylor scale and ν the kinematic viscosity.

$q = 0$ will be called normalized cumulant exponents and denoted by $\tilde{c}_p$.

The collapse of the $\tilde{\zeta}(q)$ computed from different experiments implies that the non-universal component of the $\zeta(q)$, i.e., due to the specific nature of the experimental device (turbulent jet, grid turbulence, ... but also the specific value of the necessarily finite Reynolds number), can be taken into account with a multiplicative parameter $C(R_\lambda, ...)$ only:

$$\zeta(q) = C(R_\lambda, ...)\tilde{\zeta}(q). \tag{34}$$

The value of $C(R_\lambda, ...)$ is experimentally given by the computation of $\zeta(3)$ but also receives quantitative expression for specific cases of turbulent flows [21] which are derived from a finer approximation (which includes finite Reynolds number effects) of the Kármán-Howarth equation (report as well to [44–48] which are recent works about the discrepancy between experimental third order structure functiona and the four fifths law). This topic is anyhow out of the scope of the present paper and will be discussed in a forthcoming article.

4.3 Goal of multifractal analysis in turbulence

MF analysis of turbulent velocity data aims at answering several questions. The first of those is the investigation of the dependence of the MF properties with the Reynolds number and the assessment of the universal MF description relevance. The second is the issue of the possible presence of oscillating singularities in turbulent velocity data. The last question is the discrimination between the various models proposed for the universal singularity spectrum.

All these important issues require the use of a comprehensive MF formalism (computation of the whole singularity spectrum for functions with all data of singularities) to receive clear and reliable answers.

5 Application to Fully Developed Turbulence Velocity

5.1 Experimental data and analysis details

Several sets of turbulent Eulerian velocity data are analyzed in this paper. Their characteristics are summarized in Table 1. The first data set concerns the experiment performed by Chanal et al [40]. The same experimental device has been used to generate cold helium jet with different values of the Reynolds number: $R_\lambda \simeq 90$, 210, 460 and 930. Note that these four data sets are characterized by the same integral scale. The two other data sets have been performed at the ONERA Modane wind tunnel and their Reynolds numbers are: $R_\lambda \simeq 2500$ (1986 campaign) and $R_\lambda \simeq 2000$ (1995 campaign). These two previous data sets have been made available to us by Y. Gagne (Laboratoire des Écoulements Géophysiques et Industriels, Université Joseph Fourier, INPG and CNRS, Grenoble, France).

All the data are split into series of almost 32 integral scales duration (cf., Table 1) in order to estimate the confidence intervals of the computed quantities (the confidence interval used all along this paper is the common 95% confidence interval for the empirical average estimator on N samples of a Gaussian random variable: $\pm 2\frac{\sigma}{\sqrt{N}}$ where σ is the estimated standard deviation). The Taylor hypothesis of frozen turbulence (report for instance to [49]) for the Modane wind tunnel data or its local version for the helium jet are used in order to convert the raw temporal data into spatial profiles.

Eventually the discrete wavelet used to perform all the analyses in this paper is the Daubechies wavelet [50] with 3 vanishing moments.

5.2 Effect of the length of the inertial scale range

The first step in the use of any MF formalism is to check that the computed structure functions $S(q, a)$ indeed behave like power laws. The structure functions of turbulent velocity data, computed with wavelet or increment coefficients, are known to have such a behavior within the so-called inertial range, that roughly speaking extends from the integral scale L_i down to the Taylor scale λ. The value of the integral scale is controlled by the physical processes with which the energy is injected in the turbulent flow whereas the inertial range is limited at smallest scales by dissipative effects: the viscosity becomes predominantly effective and the structure functions do not behave like power laws anymore. The extend of the inertial range is mainly controlled by the Taylor scale based Reynolds number R_λ and increases with it (the ratio of L_i to λ is proportional to R_λ according to dimensional analysis).

The DWC correctly characterize the MF properties of turbulent velocity within the inertial range: the $S^d(q, a)$ (with $q > 0$) do behave like power laws in this range as a result. Linear regressions are performed within a carefully selected scale range $[a_{min} = 2^{j_{min}}, a_{max} = 2^{j_{max}}]$ in order to compute the scaling exponents $\zeta^d(q)$, where a_{min} and a_{max} (which are close to λ and L_i, respectively) delimit the observed power laws.

The situation is actually different when using the WL. By definition the coefficient $l(j, k)$ accounts for the local properties around time $2^j k$, at scale 2^j but also at smaller scales: $2^{j'}$ with $j' < j$. Hence the $l(j, k)$ can correctly characterize the MF properties only if the $d(j', k)$ account for these properties at scale 2^j but also at smaller scale $2^{j'}$. In turn, if a power law is observed for the $S^d(q, j)$ starting at a minimal scale $2^{j_{min}}$, the $S^l(q, j)$ are expected to behave like power laws only starting at a larger scale $2^{j_{min}+m}$ with $m \geq 1$. As a consequence the range of scales which can be used to compute the $\zeta^l(q)$ is shorter than the one used to compute the $\zeta^d(q)$.

This is illustrated in Fig. 5 which shows the third order structure functions computed with the DWC ($S^d(3, j)$) and the WL ($S^l(3, j)$) from different velocity data sets performed with the same experimental device but characterized by four different Reynolds number: $R_\lambda \simeq 90$, 210, 460

and 930 (cf., Section 5.1). The inertial scale range extends toward smallest scales when R_λ increases[10]. The local exponent is defined at octave j as: $(S(3, j + 1/2) - S(3, j - 1/2))$: if $S(3, j)$ is a pure power law with exponent $\zeta(3)$ then the local exponent is constant and coincides with $\zeta(3)$, and if $S(3, j)$ behaves like a power-law over a given range the local exponent is almost constant within that range. No power law behavior is observed for $S^d(3, j)$ with $R_\lambda \simeq 90$ or $R_\lambda \simeq 210$ but with $R_\lambda \simeq 460$ and $R_\lambda \simeq 930$: the local exponent is almost constant over a sufficiently large range to perform a reliable scaling exponent computation. In contrast, $S^l(3, j)$ only clearly behaves like a power law for the highest R_λ value ($R_\lambda \simeq 930$). As a consequence $\zeta^d(3)$ can be reliably estimated for $R_\lambda \simeq 460$ but not $\zeta^l(3)$: a power law behavior is observed over almost 3 octaves for $S^d(3, j)$ but only over 1 octave for $S^l(3, j)$, thus preventing any reliable measurement. According to the heuristic discussion developed in the previous paragraph, it means that the WL at scale 2^j are mainly sensitive to the DWC at scales 2^j, 2^{j-1} and 2^{j-2} and that almost two less octaves are available for the scaling exponent computation.

This discussion illustrates one important point: if the Reynolds number is moderately large (e.g., $R_\lambda \simeq 460$ for this specific experiment), one can compute the left part only (or even the part defined by $h < h_c$) of the singularity spectrum by using the DWC but not its right part since the computation of the $\zeta^l(q)$ cannot be performed. Note that the WTMM methodology suffers from the same drawback: power laws are established with the same "scale delay" [21].

5.3 Computation of scaling exponents and cumulant exponents

The remaining of this paper will focus on data sets for which the scaling exponents $\zeta^l(q)$ and thus the MF formalism based on the WL can be reliably used, i.e., the velocity data sets corresponding to $R_\lambda \simeq 930$, 2000 and 2500 (cf., Section 5.1). Raw and normalized scaling exponents singularity spectra and cumulant exponents (cf., Section 4.2) are computed using the WL and the DWC. The scale ranges over which are performed the linear regressions are carefully chosen according to the discussion made in Section 5.2.

The computed $\zeta^l(q)$ and $\tilde{\zeta}^l(q)$ and their Legendre transforms are displayed in Figs. 6, 7, 8 and 9. The cumulants $C^l(p, a)$ computed on the data set with $R_\lambda \simeq 2000$ are plotted in Fig. 10 (similar plots are obtained with other data sets). The estimated values of the cumulant exponents c_p and $\tilde{c}_p$ are listed in Tables 3 and 4.

5.4 Discussions

5.4.1 Dependence of the singularity spectrum on the Reynolds number

The dependence of the MF properties with the Reynolds number R_λ is now discussed from the Figs. 6 and 7. A dependence with the Reynolds number is observed: the $\zeta^l(q)$ computed for the three Reynolds numbers $R_\lambda \simeq 930$, 2000 and 2500 do not coincide (note in particular that $\zeta^l(3)$ is always smaller than 1 but gets closer to 1 when R_λ increases). As a direct consequence their Legendre transforms $D^l(h)$ do not coincide and the cumulant exponents c_p^l are distinct (cf., Table 3). In contrast the normalized scaling exponents $\tilde{\zeta}^l(q)$ very clearly collapse on a common curve for the full range of computed orders q, as do their Legendre transforms. The normalized cumulant exponents $\tilde{c}_p^l$ are in a very good agreement for all data sets (cf., Table 4).

The MF properties of turbulent velocity depend on specific details of the experimental flow (for instance the Reynolds number) and are thus not universal. The MF properties of experimental data can anyway be related to those of turbulent flows with $R_\lambda \to +\infty$, which are universal, through the commonly used normalized scaling exponents as discussed in Section 4.2.

5.4.2 Investigation of the oscillating singularities existence

The methodology proposed in Section 3.4 is used to assess the existence of oscillating singularities in experimental turbulent velocity data. The Legendre transform of scaling exponents computed with the DWC ($D^d(h)$) is compared to the Legendre transform of scaling exponents computed with the WL ($D^l(h)$), in particular for h values close to the abscissa of the observed maxima (located at $h_0 \simeq 0.34$) for the data set corresponding to $R_\lambda \simeq 2000$ (see Fig. 9). $D^d(h)$ and $D^l(h)$ clearly coincide on the whole left part of the singularity spectrum: $h \leq h_0$. The same results is obtained with data sets characterized by $R_\lambda \simeq 930$ and $R_\lambda \simeq 2500$.

The interpretation of this result is that no oscillating singularity is detected in turbulent velocity with the proposed methodology. According to the discussion made in Section 3.3.2 one cannot conclude to the absence of oscillating singularities but if such singularities exist, their contribution to the MF properties is minor. As a consequence this result backs the use of MF models based on multiplicative cascades (such as the log-normal or log-Poisson discussed above) since they result in MF functions with simple singularities only.

Several works [9–12] had addressed the issue of the existence of oscillating singularities in experimental data. This is the first time that this issue receives an answer (though partial) from data analysis. This has been achieved because the WL allow to define a MF formalism valid for all kinds of singularities since they better characterize the local regularity properties (see Section 3.2.3).

---

[10] Note that the integral scale L_i of all these data sets is the same since being fixed by the experimental device.

5.4.3 Discrimination between multifractal models

This section discusses the universal MF properties of turbulent velocity data, focusing on the right part of the normalized singularity spectrum $\tilde{D}(h)$ and on the values of the normalized cumulant exponents $\tilde{c}_p$. As discussed in the Section 4.1 the computation of the right part of $\tilde{D}(h)$ ($h \geq h_0$) is essential for the discrimination between the log-normal and She-Lévêque models. Figs. 6 and 7 shows that all computed singularity spectra are in very good agreement with the log-normal model and clearly depart from the She-Lévêque model, within the confidence intervals (see Fig. 8 for $R_\lambda \simeq 2000$; similar results are obtained for $R_\lambda \simeq 930$ and 2500). Note that the log-normal model has one free parameter (c_2) which has been chosen in Figs. 6 and 7 as $c_2 = -0.025$, which is its commonly accepted value [39–41, 27] and not adjusted on order to fit the computed $\tilde{D}^l(h)$.

The normalized cumulant exponents $\tilde{c}_p^l$ are computed up to order $p = 4$ (cf., Table 4) and are found to take common values (within the confidence intervals):

$$\begin{cases} \tilde{c}_1^l \simeq & 0.372 \pm 0.004 \\ \tilde{c}_2^l \simeq & -0.025 \pm 0.002 \\ \tilde{c}_3^l \simeq & 0.000 \pm 0.001 \\ \tilde{c}_4^l \simeq & 0.000 \pm 0.001 \end{cases}$$

These values exhibit a clear agreement with the log-normal model since only $\tilde{c}_1^l$ and $\tilde{c}_2^l$ are found to have non zero values. The computed values of $\tilde{c}_1^l$ and $\tilde{c}_2^l$ furthermore satisfy the condition $\tilde{c}_1^l = 1/3 + 3/2\tilde{c}_2^l$ imposed by the log-normal model (cf. Section 4.1) and the computed value of $\tilde{c}_2^l$ coincides with previous estimation [39–41, 27]. Note that the log-normal model has been sometimes rejected arguing a violation of the Novikov's condition [51]. This wrong conclusion has been drawn assuming a quadratic behavior of the scaling exponents for all orders q, whereas the $\zeta(q)$ necessarily behave like a linear function of q beyond the critical orders q_*^+ and q_*^- (cf., Eq. (30)): the log-normal model (with $c_2 = -0.025$) actually satisfies the Novikov's condition (see [37, 21, 38] for a thorough discussion of the asymptotic linear behavior of the scaling exponents).

These results confirm those previously obtained using the WTMM methodology [39, 27, 52] but using a mathematically well-founded MF formalism: the observed universal MF properties are compatible with a log-normal model for the singularity spectrum of Eulerian turbulent velocity and are fully characterized by the value of the second order cumulant exponent: $\tilde{c}_2 \simeq -0.025 \pm 0.002$.

6 Conclusions

The MF description is one of the routes that lead toward a statistical description of turbulence within the inertial scales. It ties the scaling properties of turbulence to its local regularity properties (Section 2) and also relates the observed MF properties to the underlying multiplicative cascade structure of turbulence (Section 4). The estimation of turbulence MF properties from experimental data

thus provides meaningful inferences about the physical processes which originate turbulence. A comprehensive MF analysis of experimental data which relies on well-founded mathematical basis should hence be performed in order to unequivocally establish the MF properties of turbulent velocity and thus safely extract information about the physical processes involved in turbulent flows.

The MF formalism based on the WL [20], thoroughly described and illustrated in this paper (Section 3), is the first MF formalism to address successfully the three following requests: (1) exact computation of the whole singularity spectrum; (2) mathematically well-founded basis; and (3) validity for all kinds of singularities. The MF formalism based on the WL is applied for the first time to experimental turbulent velocity data (Section 5). Methodological aspects are first thoroughly discussed and it is shown that only velocity data with sufficiently large R_λ can be analyzed. The MF analysis of three data sets from different experimental devices and with different R_λ, thus yielding strong inferences, is then performed. The dependence of the MF properties on the specific value of R_λ is carefully described and the collapse of the normalized quantities ($\tilde{\zeta}(q)$, $\tilde{D}(h)$ and $\tilde{c}_p$) characterizing the universal part of MF properties is discussed. The issue of the existence of oscillating singularities receives for the first time a clear though partial answer: no oscillating singularities are detected, which means that oscillating singularities might exist but only if bringing a minor contribution to MF properties along the discussion made in Section 3.4. A complete and definitive answer is still to be brought to this important question and the WL might be the first step toward this achievement. Eventually the universal MF properties of turbulent velocity are compared to those of proposed MF models and are accurately parameterized with cumulant exponents up to order 4. The log-normal model is clearly shown to correctly account for all observed universal MF properties and its only free parameter is estimated: $\tilde{c}_2 = -0.025 \pm 0.002$. These results confirms those previously obtained in [27, 39–41, 52]. The contribution of this paper toward the issue of discriminating between various MF models is anyway of first importance since this is first time that a complete MF analysis is done using mathematically well-founded tools.

References

1. A.N. Kolmogorov, Dokl. Akad. Nauk SSSR **30**, 299 (1941)
2. A. Obukhov, J. Fluid Mech. **13**, 77 (1962)
3. A.N. Kolmogorov, J. Fluid Mech. **13**, 82 (1962)
4. U. Frisch, *Turbulence, the Legacy of A.N. Kolmogorov* (Cambridge University Press, 1995)
5. A. Yaglom, Dokl. Akad. Nauk. SSR **166**, 49 (1966)
6. B. Mandelbrot, J. Fluid. Mech. **62**, 331 (1974)
7. L. Richardson, *Weather prediction by numerical process* (Cambridge University Press, 1922)
8. B. Castaing, Y. Gagne, E. Hopfinger, Physica D **46**, 177 (1990)
9. J. Hunt, J. Vassilicos, Proc. R. Soc. Lond. A **434** (1991)
10. N. Kevlahan, J. Vassilicos, Proc. R. Soc. Lond. A **447**, 341 (1994)

11. A. Arneodo, E. Bacry, J. Muzy, Phys. Rev. Letters **74**, 4823 (1995)
12. A. Arneodo, E. Bacry, S. Jaffard, J. Muzy, J. Stat. Phys. **87(1–2)**, 179 (1997)
13. G. Parisi, U. Frisch, *On the singularity structure of fully developed turbulence, appendix to Fully developed turbulence and intermittency by U. Frisch*, in *Proc. Int. Summer school Phys. Enrico Fermi, North Holland* (1985)
14. S. Mallat, *A Wavelet Tour of Signal Processing* (Academic Press, San Diego, CA, 1998)
15. J. Muzy, E. Bacry, A. Arneodo, Phys. Rev Lett. **67**, 3515 (1991)
16. C. Meneveau, J. Fluid Mech. **232**, 469 (1991)
17. S. Jaffard, S.I.A.M. J. Math. Anal. **28(4)**, 944 (1997)
18. J. Muzy, E. Bacry, A. Arneodo, Phys. Rev. E **47**, 875 (1993)
19. A. Arneodo, E. Bacry, J. Muzy, Physica A **213**, 232 (1995)
20. S. Jaffard, *Wavelet Techniques in Multifractal Analysis*, in *"Fractal Geometry and Applications: A Jubilee of Benoit Mandelbrot", ed.: M. Lapidus and M. van Frankenhuysen, Proc. of Symp. in Pure Mathematics* (AMS, 2004)
21. B. Lashermes, Ph.D. thesis, École Normale Supérieure de Lyon (2005)
22. B. Lashermes, S. Jaffard, P. Abry, *Wavelet Leaders Based Multifractal Analysis*, in *ICASSP 2005 Conference, Philadelphia, USA* (2005)
23. S. Jaffard, B. Lashermes, P. Abry, *Wavelet leaders in Multifractal Analysis*, in *WAA05 (4th Int. Conference on Wavelet Analysis and its Applications), Macau, China* (2005)
24. M. Schroeder, *Fractals, Chaos, Power Laws. Minutes from an Infinite Paradise* (W.H. Freeman and Company, 1991)
25. A.N. Kolmogorov, Dokl. Akad. Nauk SSSR **32**, 16 (1941)
26. A. Arneodo, S. Manneville, J. Muzy, Eur. Phys. J. B **1**, 129 (1998)
27. J. Delour, J. Muzy, A. Arneodo, Eur. Phys. J. B **23**, 243 (2001)
28. V. Venugopal, S. Roux, E. Foufoula-Georgiou, A. Arneodo, Water Resour. Res. **42** (2006)
29. B. Lashermes, E. Foufoula-Georgiou, submitted to Water Resour. Res. (2007)
30. A. Arneodo, E. Bacry, J. Muzy, J. Math. Phys. **39**(8), 4142 (1998)
31. S. Jaffard, Y. Meyer, Memoirs of the AMS. **123** (1996)
32. S. Jaffard, J. Math. Phys. **39**, 4129 (1998)
33. Z.S. She, E. Lévêque, Phys. Rev. Letters **72**, 336 (1994)
34. B. Castaing, B. Dubrulle, J. Phys. II France **5**, 895 (1995)
35. E. Novikov, Phys. Rev. E **50**, R3303 (1994)
36. B. Dubrulle, Phys. Rev. Lett. **73**, 959 (1994)
37. B. Lashermes, P. Abry, P. Chainais, Int. J. of Wavelets, Multiresolution and Information Processing **2**(4), 497 (2004)
38. B. Lashermes, P. Abry, submitted to Eur. Phys. J. B (2007)
39. A. Arneodo, E. Bacry, S. Jaffard, J. Muzy, J. Four. Anal. Appl. **4**, 159 (1998)
40. O. Chanal, B. Chabaud, B. Castaing, B. Hébral, Eur. Phys. J. B **17**, 309 (2000)
41. Y. Malécot, C. Auriault, H. Kahalerras, Y. Gagne, O. Chanal, B. Chabaud, B. Castaing, Eur. Phys. J. B **16**, 549 (2000)
42. T. von Kármán, L. Howarth, Proc. Roy. Soc. **A164 917** (1938)
43. A. Arneodo, C. Baudet, F. Belin, R. Benzi, B. Castaing, B. Chabaud, R. Chavarria, S. Ciliberto, R. Camussi, F. Chillà et al., Europhys. Lett. **34**, 411 (1996)
44. E. Lindborg, Phys. of Fluids **11**, 510 (1999)
45. L. Danaila, F. Anselmet, T. Zhou, R. Antonia, J. Fluid Mech. **391**, 359 (1999)
46. F. Moisy, P. Tabeling, H. Willaime, Phys. Rev. Lett. **82**, 3994 (1999)
47. T. Lundgren, Phys. of Fluids **14**, 638 (2002)
48. Y. Gagne, B. Castaing, C. Baudet, Y. Malécot, Phys. of Fluids **16**, 482 (2004)
49. H. Tennekes, J. Lumley, *A First Course in Turbulence* (MIT Press, 1972)
50. I. Daubechies, Comm. Pure and App. Math. **41**, 909 (1988)
51. E. Novikov, Prikl. Math. Mekh. **35**, 266 (1970)
52. S. Roux, Ph.D. thesis, Université d'Aix-Marseille II (1996)

R_λ	$\simeq 90$	$\simeq 210$	$\simeq 460$	$\simeq 930$	$\simeq 2000$	$\simeq 2500$
total duration (in integral scale)	$\simeq 96000$	$\simeq 49000$	$\simeq 29000$	$\simeq 8000$	$\simeq 2000$	$\simeq 900$
number of series	3024	1532	892	248	64	27
serie duration (in integral scale)	$\simeq 32$	$\simeq 32$	$\simeq 32$	$\simeq 32$	$\simeq 32$	$\simeq 32$

Table 1. Experimental data details

model	c_1	c_2	c_3	c_4
log-normal	$\simeq 0.371$	-0.025	0	0
She-Lévêquel	$\simeq 0.381$	$\simeq -0.0365$	$\simeq 0.00494$	$\simeq -0.000667$

Table 2. Cumulant exponents of the log-normal (with the commonly accepted value: $c_2 = -0.02$) and She-Lévêque models.

R_λ	c_1^l	c_2^l	c_3^l	c_4^l
$\simeq 930$	0.334 ± 0.002	-0.023 ± 0.001	0.0000 ± 0.0003	-0.0003 ± 0.0002
$\simeq 2000$	0.341 ± 0.003	-0.022 ± 0.001	-0.0001 ± 0.0006	-0.0002 ± 0.0004
$\simeq 2500$	0.349 ± 0.004	-0.024 ± 0.002	0.000 ± 0.001	0.000 ± 0.001

Table 3. Cumulant exponents computed with the WL.

R_λ	$\tilde{c}_1^l$	$\tilde{c}_2^l$	$\tilde{c}_3^l$	$\tilde{c}_4^l$
$\simeq 930$	0.373 ± 0.002	-0.026 ± 0.001	0.0001 ± 0.0003	-0.0003 ± 0.0002
$\simeq 2000$	0.370 ± 0.003	-0.024 ± 0.002	-0.000 ± 0.001	-0.0003 ± 0.0004
$\simeq 2500$	0.373 ± 0.004	-0.026 ± 0.002	0.000 ± 0.001	0.000 ± 0.001

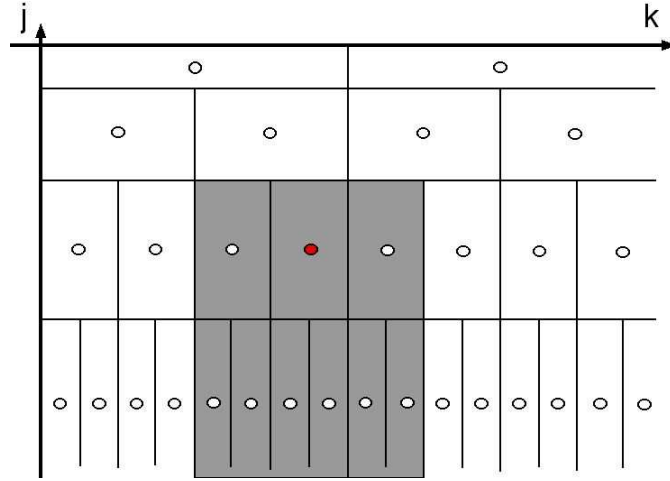**Table 4.** Normalized cumulant exponents computed with the WL.

Fig. 1. Space-scale plane and the dyadic grid. Every dot (∘) represents a discrete wavelet coefficient $d(j,k)$ and the surronding rectangle the dyadic interval $\lambda(j,k)$. The dashed area sketches the subset $3\lambda(j,k)$ associated to the wavelet leader $l(j,k)$ (solid dot •).
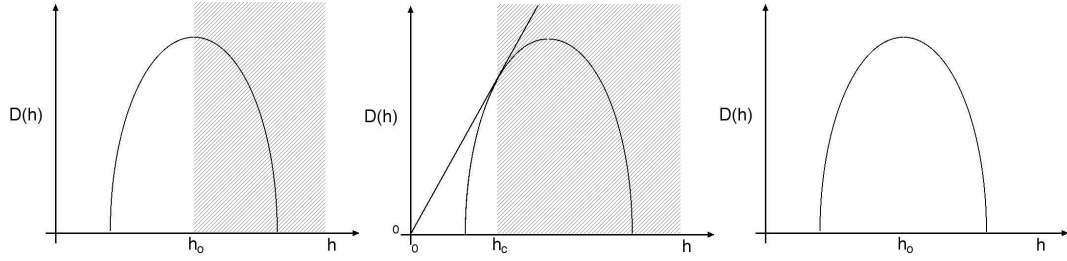

Fig. 2. Multifractal formalism validity. Domains of validity (white area) and of non-validity (dashed ares) of the MF formalism based on the DWC for uniform Hölder functions with only simple singularities (left), for all uniform Hölder functions (middle) and of the MF formalism based on the WL (right).
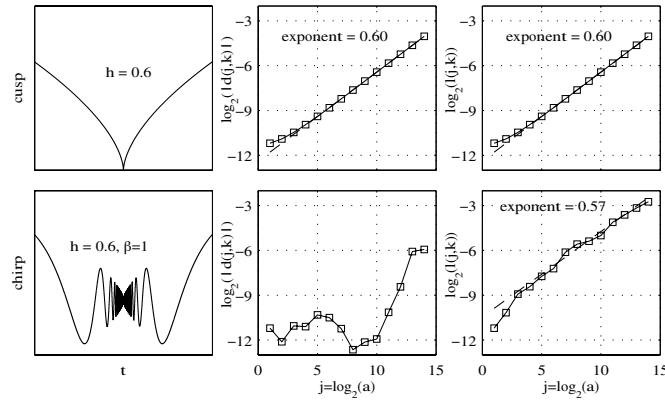
Fig. 3. Simple vs. oscillating singularities. DWC $d(j,k)$ and WL $l(j,k)$ computed with the cusp: $|x-x_0|^{0.6}$ (top) and with the chirp: $|x-x_0|^{0.6}\sin\left(\frac{1}{|x-x_0|^1}\right)$ (bottom) and plotted in a $\log_2 - \log_2$ diagram (k is chosen such that $0 \in \lambda(j,k)$). Daubechies wavelet with order 1 is used.
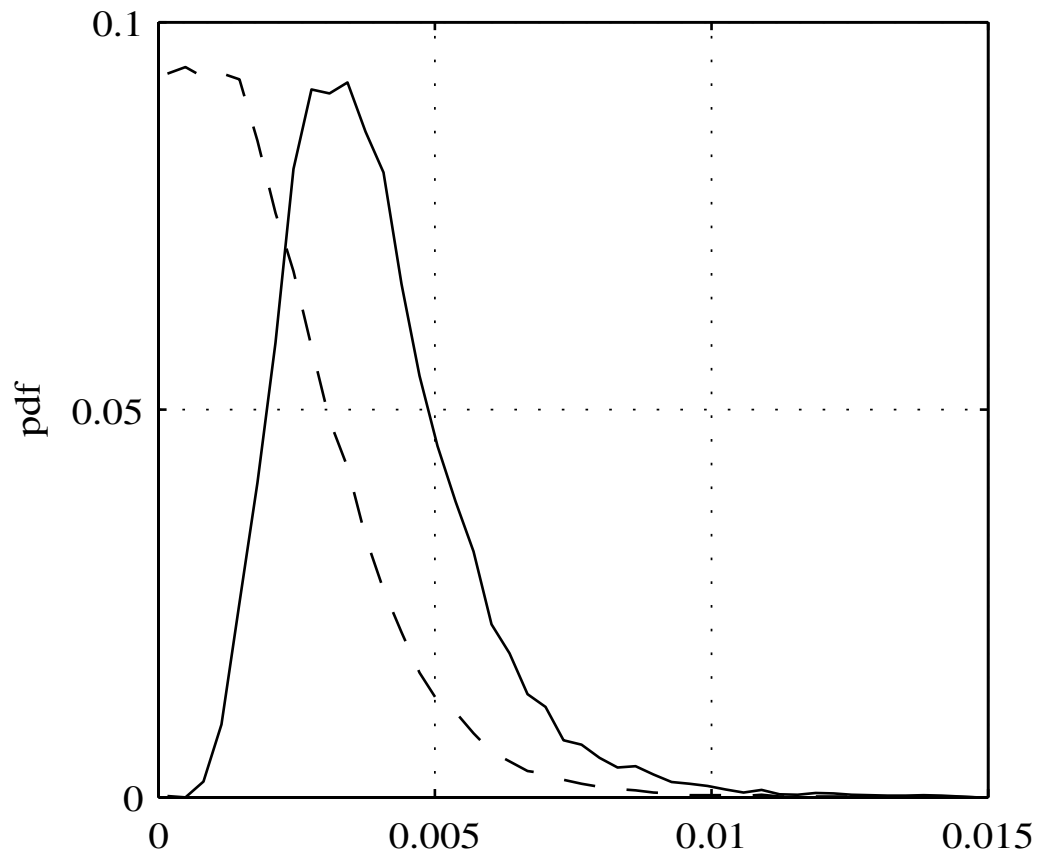
Fig. 4. Histograms of the WL (solid line) and of the absolute value of the DWC (dashed line) computed on a realization of the random wavelet cascade.
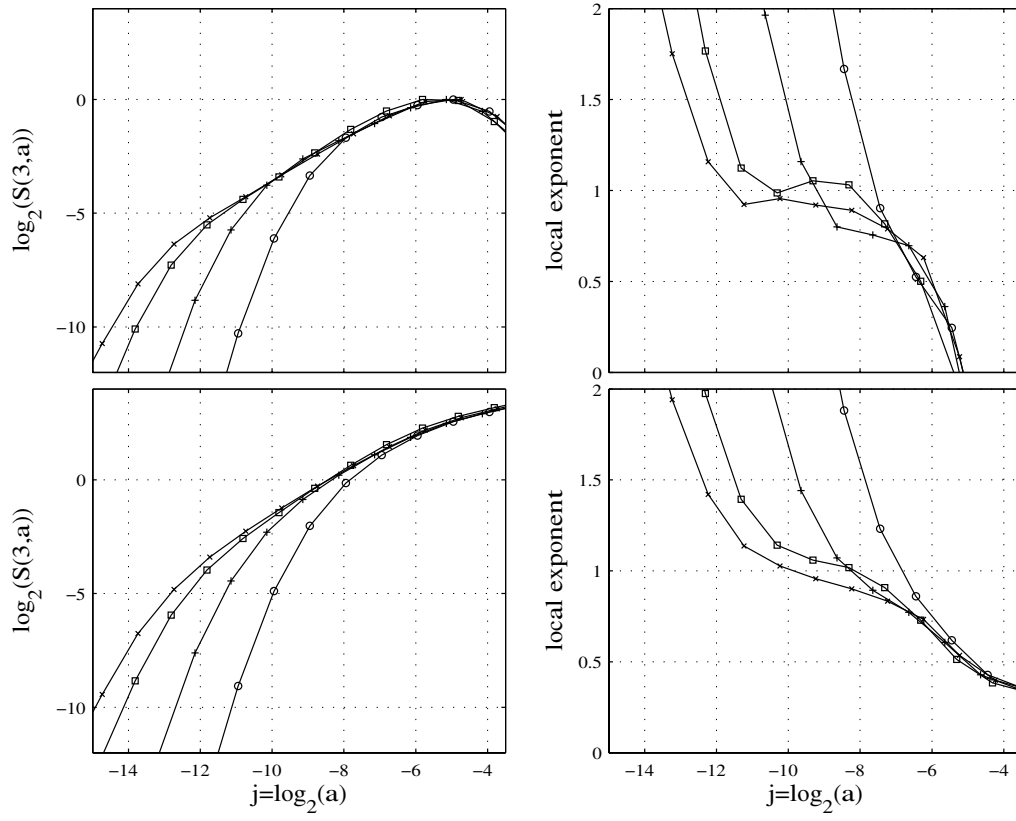
Fig. 5. Dependence of the third order structure function on R_λ. Third order structure functions (left) built with the DWC (top) and the WL (bottom) and corresponding local exponent (right): $R_\lambda \simeq 90$ (o), $R_\lambda \simeq 210$ (+), $R_\lambda \simeq 460$ (□) and $R_\lambda \simeq 930$ (×). The scale $a = 2^j$ is in meters.
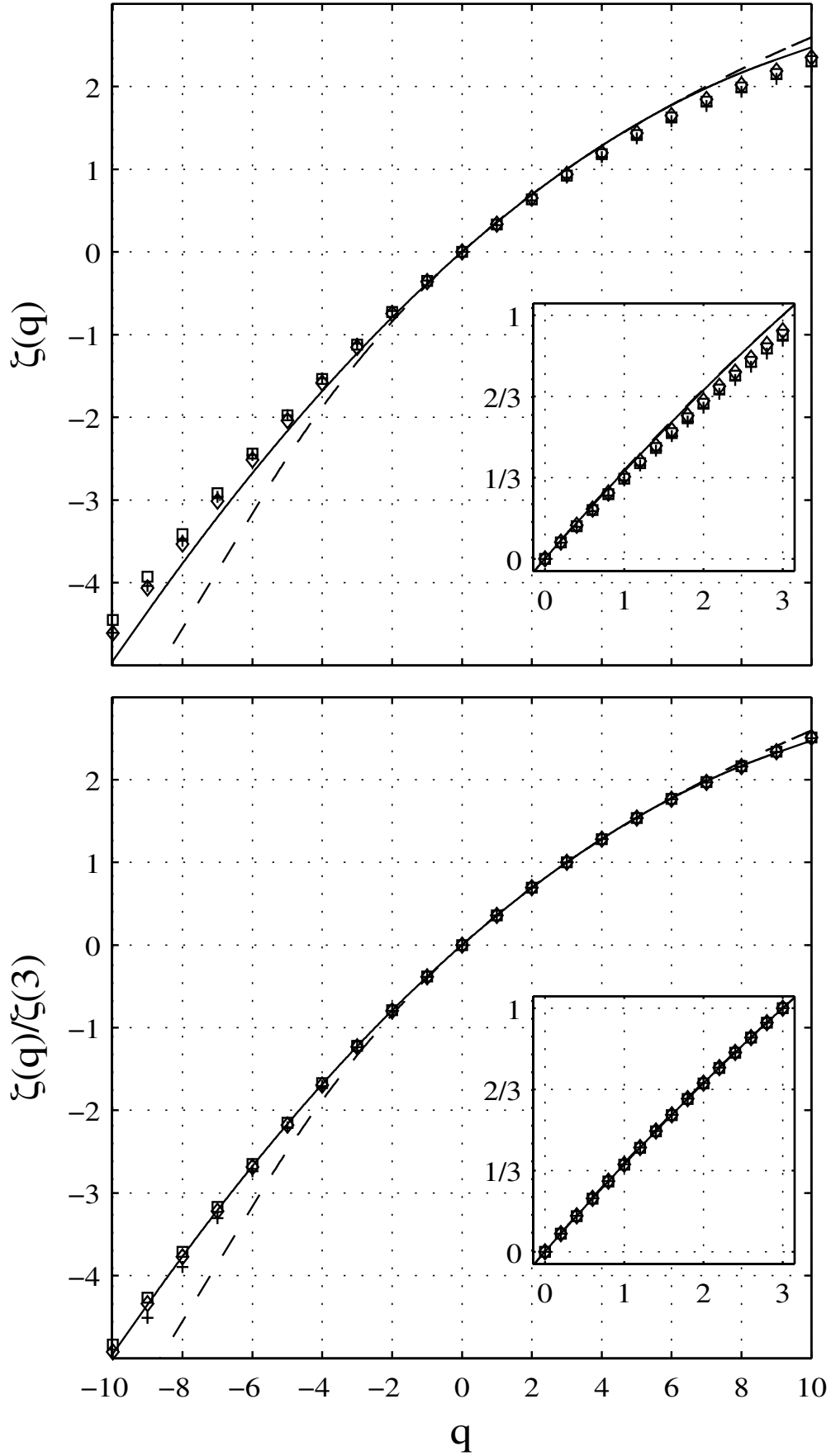
Fig. 6. Raw scaling exponents $\zeta^l(q)$ **and normalized scaling exponents** $\tilde{\zeta}^l(q)$. $R_\lambda \simeq 930$ (+), $R_\lambda \simeq 2000$ (□) and $R_\lambda \simeq 2500$ (◇). Log-normal (solid line) and She-Lévêque (dashed line) models are plotted.
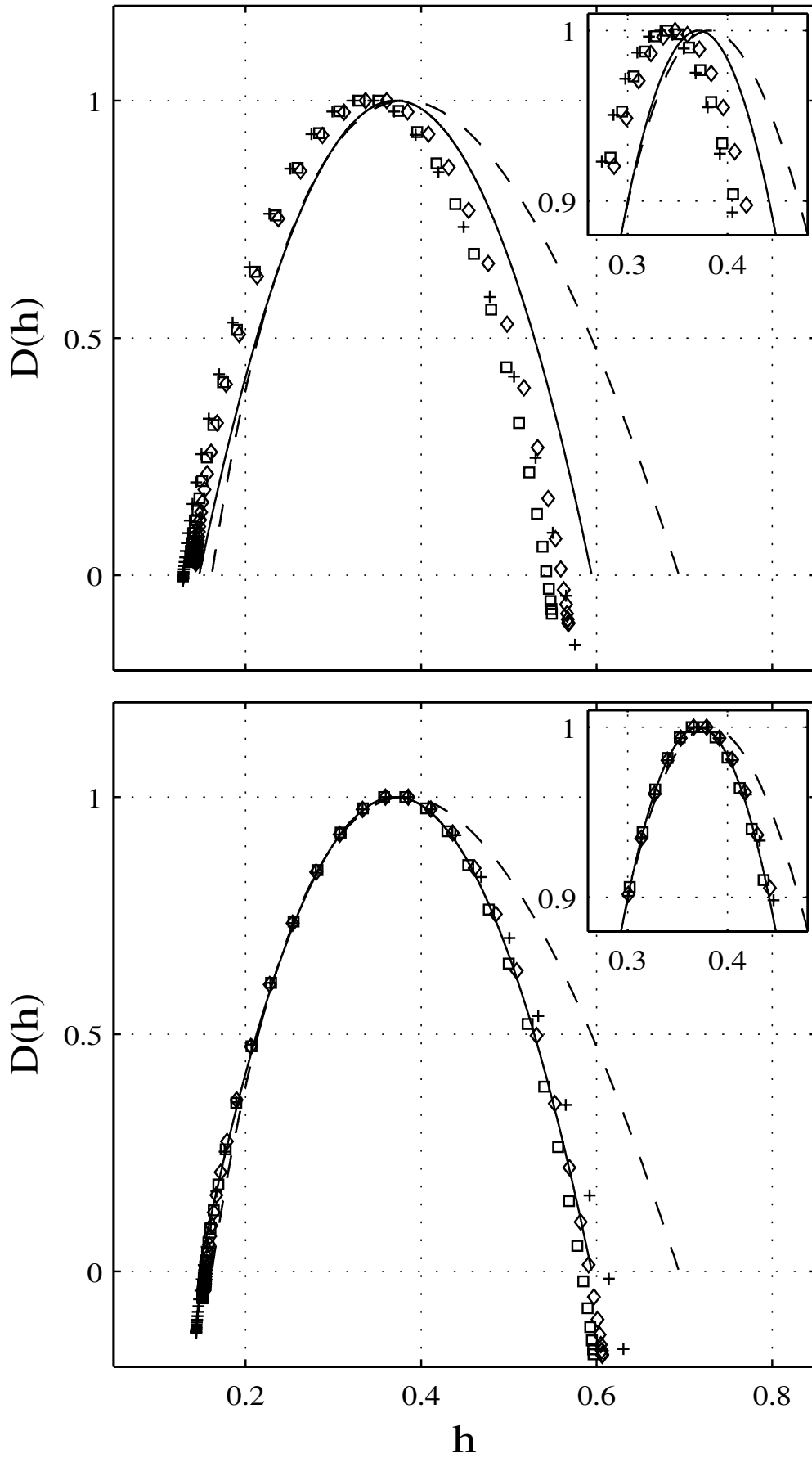
Fig. 7. Legendre transforms of the $\zeta^l(q)$ **and the** $\tilde{\zeta}^l(q)$**.** $R_\lambda \simeq 930$ (+), $R_\lambda \simeq 2000$ (□) and $R_\lambda \simeq 2500$ (◇). Log-normal (solid line) and She-Lévêque (dashed line) models are plotted.
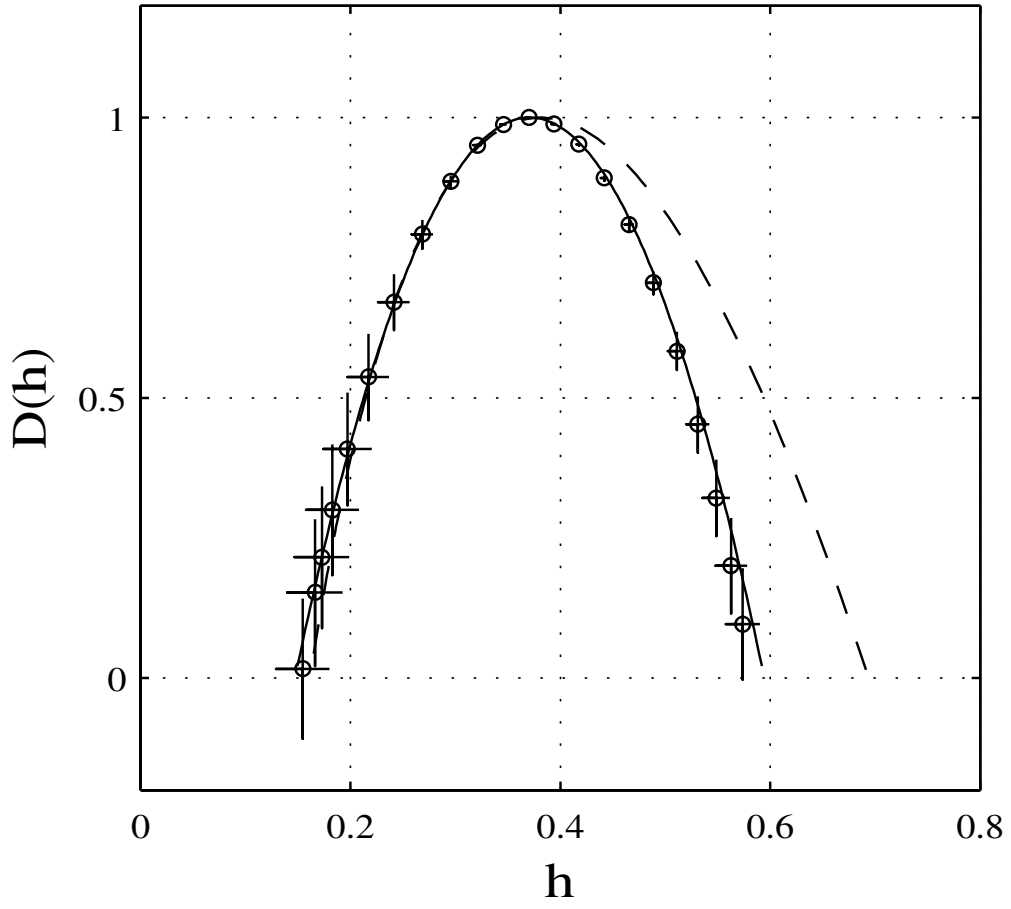
Fig. 8. $R_\lambda \simeq 2000.$ Singularity spectrum computed with the WL (o) and computed confidence intervals.
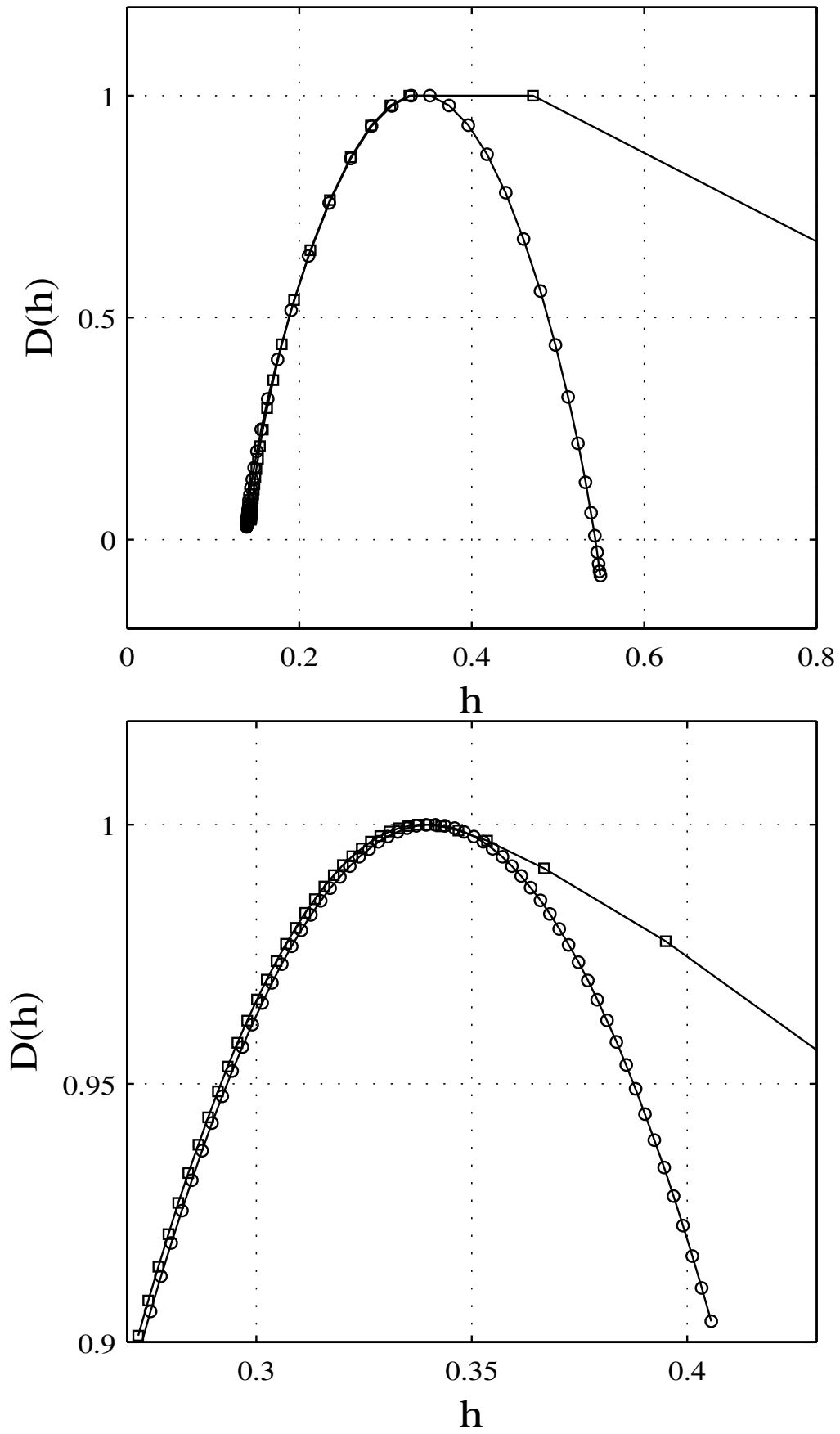
Fig. 9. $R_\lambda \simeq 2000$. Singularity spectra computed with the DWC ($\square$) and the WL (o).

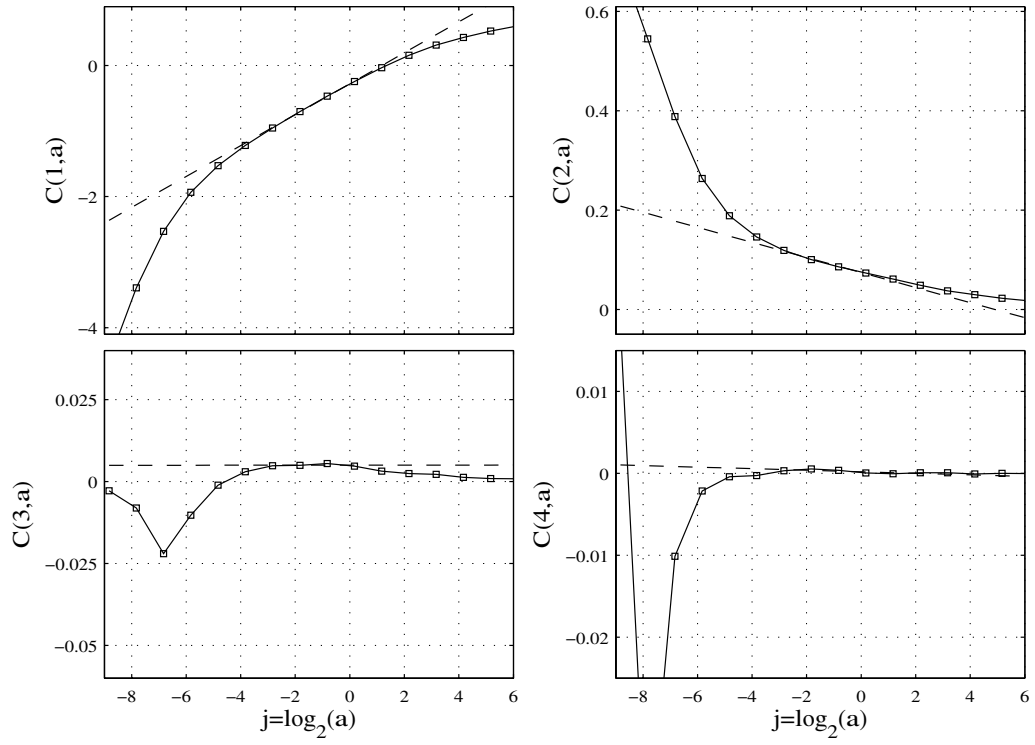**Fig. 10.** $R_\lambda \simeq 2000$**, cumulant analysis.** $C^l(1,a)$ (top left), $C^l(2,a)$ (top right), $C^l(2,a)$ (bottom left) or $C^l(4,a)$. The scale $a = 2^j$ is in meters.